

## CHARACTERIZING THE ANGULAR DISTRIBUTION OF AN LED-BASED SOLAR SIMULATOR FOR PV MODULES

Riechelmann, Stefan<sup>1</sup>

<sup>1</sup>Physikalisch-Technische Bundesanstalt (PTB), Bundesallee 100, D-38116 Braunschweig, Germany

**ABSTRACT:** Solar simulators for PV modules often consist of several lamps arranged side by side to provide the irradiance necessary for PV module testing under standard test conditions. Since these simulators are no point sources, the angular distribution of the radiance emitted by the simulators can lead to systematic deviations in measured PV device's performances. To quantify the opening angle of a solar simulator, pictures of a digital single-lens reflex (DSLR) camera and irradiance measurements of a CCD-array spectroradiometer were combined to derive its approximate spectral radiance distribution. We applied our technique to an LED-based solar simulator, where the radiance of 18 different LED colors could be examined separately and thus an approximation of the spectral radiance emitted by the simulator can be made. An angle of incidence of  $15.6^\circ$  has been observed for this system at the center of a PV module, raising to about  $21.5^\circ$  towards the edge of the test plane.

**Keywords:** characterization, calibration, solar simulator

### 1 INTRODUCTION

A secondary calibration of PV modules is commonly performed with solar simulators that show a wide range of different designs. This results in a wide variation of the angle of incidence in which light is received by a module under test. The angular distribution of the light field of a solar simulator is one of the crucial input parameters necessary for performing an angular mismatch correction for a PV device calibration [1]. It is possible to characterize the radiance field emitted by the solar simulator by sampling the solar simulator point by point with a scanning spectroradiometer [1]. However, a complete sampling is time consuming and the angular resolution is will be quite low compared to the camera-based approach we proposed earlier in [2]. Capturing the light source with a DSLR camera provides a high angular resolution of the light field and a fast measuring rate, enabling us to perform the measurement at different positions of the solar module in little additional time. The method gives users a cost-effective way to characterize the angular behavior of their system and helps solar simulator manufacturers to fast-check their system during design optimization cycles.

### 2 APPROACH

The basic approach of our camera-based method has been first described in [3]. Compared to the previous publication, additional correction steps to the raw camera pictures (Figure 1) are performed and spectral irradiance measurements are added to the method. We also show the possibilities to derive spectral radiance of a module-sized LED-based solar simulator, the overhauled method is described in detailed steps below:

- 1) The DSLR camera is placed in the test plane of the solar simulator, a photo of each of the 18 LED color channels  $k$  is taken, providing count values  $P_k(x,y,z)$  in raw picture format.
- 2)  $P_k(x,y,z)$  is corrected for lens distortion, vignetting and dark current. In addition, a blurring filter is applied, to not loose information due to interpolation.
- 3) The metric grid is scaled to the width  $x$  and height  $y$  of the simulator by detecting AR markers placed at the corners of its frame [4] and the distance  $z$  between its emitting surface and the test plane.

- 4) With known  $x$ ,  $y$  and  $z$  the  $P_k(x,y,z)$  are converted and interpolated to a polar coordinate grid with  $0.1^\circ$  step size:

$$\begin{aligned} r_i &= \sqrt{x_i^2 + y_i^2 + z^2}, \\ \theta_i &= \arccos\left(\frac{z}{r_i}\right), \\ \varphi_i &= \arctan2\left(\frac{y_i}{x_i}\right). \end{aligned}$$

- 5)  $P_k(\theta, \varphi)$  is now scaled as follows:

$$P_{k,rel}(\theta, \varphi) = \frac{P_k(\theta, \varphi)}{\iint_{\Omega} P_k(\theta, \varphi) \cdot \cos \theta \cdot d\Omega},$$

this way a spatial distribution  $P_{k,rel}(\theta, \varphi)$  that is proportional to the radiance is provided.

- 6) Spectral irradiance  $E_{k,\lambda}(\lambda)$  is measured with an CCD-array spectroradiometer for each of the 18 LED channels  $k$  separately.
- 7) When using the simulator for PV module calibrations, all LED channels are turned on simultaneously with channel-wise different power values, so their individual spectra add up to an AM1.5 spectrum  $E_\lambda(\lambda)$ . Since the LED spectra overlap, a proportion factor  $PF_{k,\lambda}$  is calculated, stating how much LED channel  $k$  contributes to  $E_\lambda$  at wavelength  $\lambda$ :

$$PF_{k,\lambda}(\lambda) = \frac{E_{k,\lambda}}{E_\lambda}.$$

- 8) With  $PF_{k,\lambda}(\lambda)$  known, the spectral radiance field of the simulator can be calculated as follows:

$$L_\lambda(\lambda, \theta, \varphi) = \sum_{k=1}^{18} E_\lambda(\lambda) \cdot PF_{k,\lambda}(\lambda) \cdot P_{k,rel}(\theta, \varphi).$$

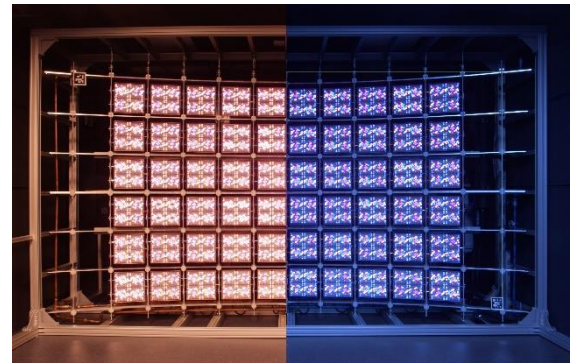


**Figure 1:** Composite picture of the LED-based solar simulator with all 18 LEDs turned on. Left: Uncorrected RAW picture. Right: Vignetting- and distortion-corrected picture.

In addition, we improved several technical aspects of our measuring procedure: Originally, we used a high camera exposure time combined with the 10 ms long flash of a xenon simulator to synchronize the measurements. Since flashes of the LED-based solar simulator are much longer, we now synchronize the measurement by flashing for two seconds and using a sufficiently low exposure time to avoid saturation. We also removed the built-in IR filter of our camera to capture radiances with wavelengths up to 1100 nm. As input values for the vignetting correction, an opaque glass is placed directly on top of the camera objective and a photo is taken. The count value of a pixel is then related to the distance of the pixel to the middle of the picture and the corresponding set of values is fitted by a polynomial function which is used inversely for correction of the vignetting (Figure 2).

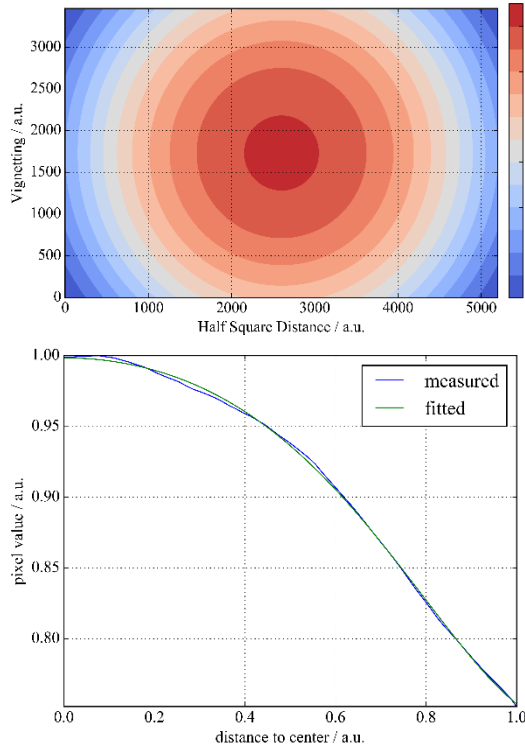


**Figure 2:** Upper plot: Normalized count values of a picture taken with an opaque glass on top of the camera objective. Lower plot: Normalized count values are shown in dependence of distance to the picture middle. A correction polynomial is fitted towards these values and used for vignetting correction.

Since our simulator has small but bright LED spots in the picture, special emphasis must be given on containing the information of the spots while performing the interpolation to a regular polar grid. Therefore, an intentional blurring over 10 x 10 pixels of the picture has been performed.

Our LED-based solar simulator gives the possibility to derive spectral information by combining pictures of individual tunable LED channels and spectroradiometer measurements. However, this is not possible in case of broadband light sources. In this case a set of bandpass filters put sequentially in front of the camera could be used to apply the same metric to derive spectral radiance.

### 3 MEASUREMENTS AND RESULTS

The emitted radiance field of an LED-based solar simulator at two different positions of the light field has been examined with the proposed method. Placing the camera at a central position in the test plane gives the spectral radiance distribution shown in Figure 3. At 775 nm, the radiance is provided by several LEDs showing an overlapping emission spectrum: LED 7 provides 5 %, LED 11 69 %, LED 12 17 % and LED 13 7 % to the integral of the radiance at that wavelength. When repeating the measurement at the upper left edge of a PV module, the most radiance originates due to geometrical reasons from the lower right of the field of view (Figure 4).

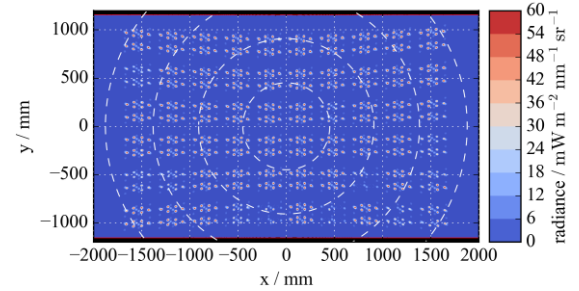


**Figure 3:** Spectral radiance emitted by the LED-based solar simulator, perceived by the middle spot of a PV module.

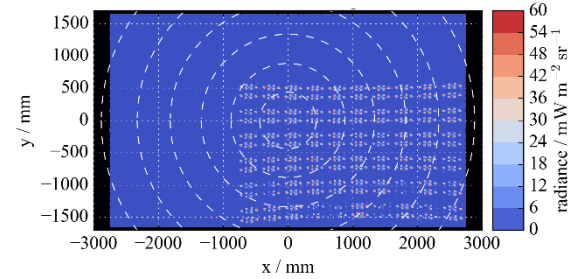


**Figure 4:** Spectral radiance perceived by the upper left edge of a solar module.

The radiance is now integrated ring-wise in  $1^\circ$  steps, beginning from the middle of the field of view, and accumulating the values from angle to angle. This way it can be derived how much irradiance originates from which angle of incidence (Figure 5). In our case, 80 % of the irradiance comes from within an angle of incidence of  $15.6^\circ$  at the center of a PV module. Towards the edge of a PV module, the angle of incidence raises up to  $21.5^\circ$ . When calculating the angle of incidence for each wavelength of the spectral radiance, it is also possible to check for wavelength-dependent variations (Figure 6). Our solar simulator shows only small variations from  $15.4^\circ$  to  $15.8^\circ$  over its wavelength range for the center of a PV module but  $20.8^\circ$  to  $22.4^\circ$  at the edge of a PV module.

### 4 SUMMARY

A camera-based method for the determination of the spectral radiance emitted by a LED-based solar simulator for PV modules is presented. Measurements were performed at the center and the edge of a PV module area, showing a spectral and spatial dependency of the opening angle ranging from  $15.4^\circ$  at the center of the PV module up to  $22.4^\circ$  at the edge of the test plane.

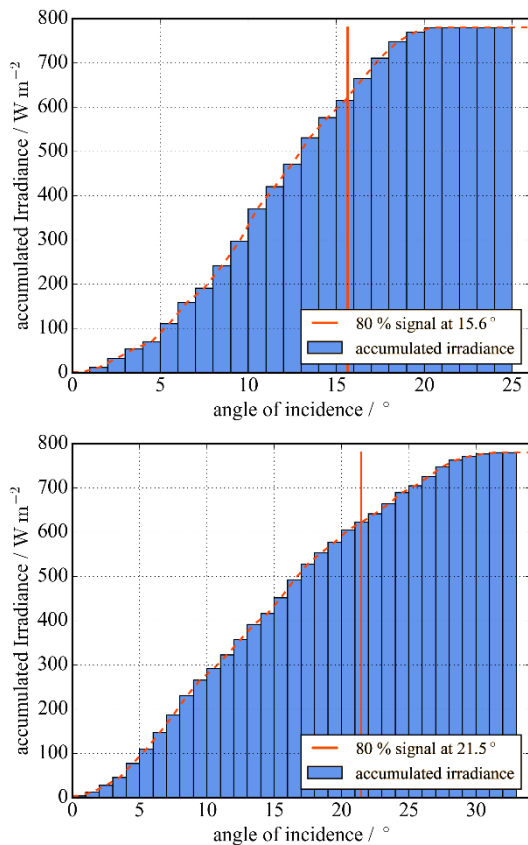


**Figure 5:** Histogram that shows how much irradiance originates from a certain angle of incidence at the center (upper plot) and edge (lower plot) of a solar module.

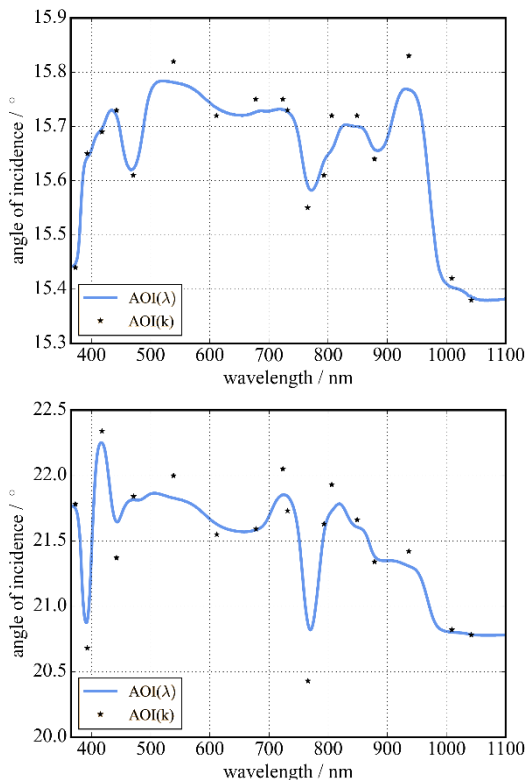


**Figure 6:** Wavelength-dependent angle of incidence, derived from spectral radiance of the LED-based solar simulator at the center (upper plot) and edge (lower plot) of a PV module.

## 5 ACKNOWLEDGEMENT

This project (PV-Enerate) has received funding from the EMPIR programme co-financed by the Participating States and from the European Union's Horizon 2020 research and innovation programme. Furthermore, the authors acknowledge financial support of the MNPQ-Program provided by the German Federal Ministry of Economic Affairs and Energy.

## 6 REFERENCES

- [1] F. Plag, I. Kröger, S. Riechelmann, and S. Winter, Multidimensional model to correct PV device performance measurements taken under diffuse irradiation to reference conditions, *Solar Energy* 174, 431–444 (2018).
- [2] F. Plag et al., Comprehensive Analysis of a Pulsed Solar Simulator to Determine Measurement Uncertainty Components. Amsterdam: (2014). Proceedings of 29th European Photovoltaic Solar Energy Conference and Exhibition. pp. 2435 - 2442.
- [3] S. Riechelmann and F. Plag, eds., A Camera-Based Characterization Method for Solar Simulators // 33rd European Photovoltaic Solar Energy Conference and Exhibition. Proceedings of the international conference held in Amsterdam, The Netherlands, 25 September-29 September 2017 (WIP, 2017).
- [4] H. Kato and M. Billingham, Marker tracking and HMD calibration for a video-based augmented reality conferencing system, in Proceedings 2nd IEEE and ACM International Workshop on Augmented Reality (IWAR'99) (IEEE Comput. Soc, 1999), pp. 85–94.